Vol. 90: 141–156, 2024
https://doi.org/10.3354/ame02013

AQUATIC MICROBIAL ECOLOGY
Aquat Microb Ecol

Published October 10

Mortality partitioning between viral lysis and microzooplankton grazing in successive phytoplankton blooms using dilution and molecular methods

Kyle M. J. Mayers[1,*], Katrine Sandnes Skaar[1], Sigrid Mugu[1], Elizabeth L. Harvey[2], Aud Larsen[1]

[1]NORCE Norwegian Research Centre, Bergen 5008, Norway
[2]Department of Biological Sciences, University of New Hampshire, Durham, NH 03824, USA

ABSTRACT: Phytoplankton play crucial roles in aquatic ecosystems, serving as the foundation of marine food webs and being responsible for ~50% of the world's oxygen production. Predation by microzooplankton and viral lysis are the major sources of phytoplankton mortality, with the balance between these 2 processes affecting microbial food webs and biogeochemical cycles. However, determining the dominant mortality process in time and space remains an open question. This study investigated microzooplankton grazing and viral lysis rates during a mesocosm experiment in western Norway. High-resolution measurements were determined on phytoplankton groups using flow cytometry to observe changes in mortality rates and carbon flow during phytoplankton blooms. Digital droplet PCR was employed to detect *Emiliania huxleyi* and *Micromonas* spp. and associated viruses within environmental samples, to explore its use for determining mortality processes and understanding the impact on the phytoplankton community. The results showed that grazing and viral lysis dominated mortality at different times, with only one significant instance of both processes being observed. Microzooplankton grazing primarily affected picoplankton, while nanoeukaryotes and *E. huxleyi* were more susceptible to viral lysis. Molecular detection did not always match with abundances or rates determined by flow cytometry; however, it did provide insights into their dynamics throughout the mesocosm. These findings provide insights into the complex interactions between microzooplankton, viruses and phytoplankton communities. Understanding the balance between microzooplankton grazing and viral lysis can contribute to a more comprehensive understanding of carbon flow in aquatic ecosystems, which has significant implications for food webs and biogeochemical cycles.

KEY WORDS: Phytoplankton · Microzooplankton · Virus · Predator–prey · Biogeochemistry · Droplet digital PCR · ddPCR · Coccolithophore

1. INTRODUCTION

Phytoplankton are an essential component of marine ecosystems, forming the base of marine food webs as well as producing ~50% of the world's oxygen and regulating global biogeochemical cycles. Factors influencing the population dynamics of phytoplankton will impact these essential biogeochemical processes. For marine phytoplankton, the major sources of mortality are predation by microbial grazers (microzooplankton) and viral lysis (Calbet & Landry 2004, Suttle 2005). Whether organisms are grazed or lysed has important implications for microbial food webs and biogeochemical cycles. Phytoplankton production by microzooplankton is hypothesized to result in high recycling within the upper ocean, due to an extended

*Corresponding author: kyma@norceresearch.no

Publisher: Inter-Research · www.int-res.com

food web, compared with larger zooplankton predators. However, many microzooplankton are a key food source for mesozooplankton (Calbet & Saiz, 2005) allowing subsequent transfer through the food web. Lysis due to viral infection releases cellular contents which when utilized by heterotrophic microbes, causes retention of carbon in the upper water column, a process termed the 'viral shunt' (Suttle 2005). Conversely, certain phytoplankton taxa contribute to the production of sticky excretions known as transparent exopolymer particles (TEPs), so that when cell lysis occurs this is released into the water column, causing enhanced aggregation of material (Guidi et al. 2016) and increased export of organic matter out of the euphotic zone; termed the 'virus shuttle' (Laber et al. 2018). However, exactly which process dominates mortality in time and space remains an open and important question.

Microzooplankton grazers and marine viruses are estimated to remove, respectively, 49–77% and 6–26% of photosynthetic biomass daily (Wilhelm & Suttle 1999, Calbet & Landry 2004, Schmoker et al. 2013). Viruses are typically specific to species or strains of phytoplankton (Nagasaki et al. 2005) and contact with the host is required for infection, so abundances of specific host and virus in the environment will impact both encounter and lysis rates. Microzooplankton are more general predators. They also require contact with the host but do show preferences for specific phytoplankton based on size class (Gonzalez et al. 1990), surface properties (Monger et al. 1999) or chemical composition (Irigoien et al. 2005), but are generally not believed to target certain species in the same way as viruses. However, viral infection can alter traits, such as the chemical composition of phytoplankton (Vardi et al. 2009, Hunter et al. 2015, Goode et al. 2019), metabolic demand (Howard-Varona et al. 2022) or their size (Evans & Wilson 2008), and thus affect the interaction between predator and prey in a mixed community.

Lab experiments examining how mortality is partitioned have been conducted with cultures of the bloom-forming coccolithophore *Emiliania huxleyi*. This organism contributes to carbon cycling through the production and release of calcium carbonate plates known as coccoliths, which can aid in the ballasting of material (Klaas & Archer 2002, Balch et al. 2016). It was suggested that virally infected *E. huxleyi* are grazed at higher rates than non-infected cells (Evans & Wilson 2008), due to the enhanced size of infected cells. Conversely, lower grazing rates on virally infected cells has also been observed, with microzooplankton being able to maintain similar growth rates due to the greater cell volume of infected prey (Goode et al. 2019).

Mortality rates in natural systems can vary in both space and time. For instance, in small picoeukaryotes, such as the ecologically important and abundant *Micromonas* spp. (Not et al. 2004, Lovejoy et al. 2007), mortality is generally dominated by microzooplankton predation rather than viral lysis (Evans et al. 2003, Baudoux et al. 2008, Anderson & Harvey 2019). However, at times of high abundance, for instance during a bloom (Evans et al. 2003) or even geographically (Baudoux et al. 2008), viral lysis can account for a greater mortality fraction. These rates can also vary over short time scales. Across a 3 d bloom, viral lysis and microzooplankton predation rates ranged from 9 to 25% and 24 to 28%, respectively (Evans et al. 2003).

Flow cytometry can allow us to determine rate measurements on different groups of phytoplankton based on size, pigmentation or other cellular features (e.g. presence of coccoliths) (Larsen et al. 2004). However, the groupings can be coarse, for instance picoeukaryotes and nanoeukaryotes can be composed of many different phylogenetic groups (Marie et al. 2010, de-Vargas et al. 2015). Molecular techniques, such as targeted quantitative PCR, can detect organisms at high taxonomic resolution, to genus or even species level. Newer methods, such as droplet digital PCR (ddPCR), can quantify target gene copies at low abundances, and better handle PCR inhibitors which can be present in environmental samples (Hindson et al. 2011, Kokkoris et al. 2021). The bloom-forming algal taxa *Micromonas* spp. and *E. huxleyi* are both commonly observed in fjord and coastal waters during spring (Larsen et al. 2004, Widdicombe et al. 2010), have extensive distributions within the world's oceans (Winter et al. 2014, Demory et al. 2019), and have well-characterised host–virus systems. This makes them an excellent target for ddPCR quantification of dynamics.

Here, we display high-resolution rate measurements of phytoplankton-group-specific grazing and viral lysis rates determined during a mesocosm experiment in June 2018. Rapid shifts in grazing and viral lysis are demonstrated for different groups identified using flow cytometry. To delve deeper into the dynamics of the important bloom-forming taxa *E. huxleyi* and *Micromonas* spp., we employed ddPCR (Hindson et al. 2011) to quantify the absolute DNA concentration of these organisms and associated viruses within incubations throughout the mesocosm experiment. By coupling ddPCR with flow cytometry data, we aimed to gain a comprehensive understanding of how grazing and viral lysis impacts the abundance and dynamics of these 2 phytoplankton species.

The main objectives of this study were to (1) observe how mortality rates by microzooplankton grazing or viral lysis change throughout mesocosm blooms on specific groups and how this may influence the flow of carbon in the pelagic environment; and (2) determine if we could use a novel molecular technique (ddPCR) to detect prey organisms within predator size fractions (>20 µm) and virus within prey size fractions (>0.6–20 µm).

2. MATERIALS AND METHODS

2.1. Mesocosm setup

Mesocosm experiments were conducted in Raunefjorden at the Espegrend Marine biological field station near Bergen, Norway (60° 16′ 11″ N, 5° 13′ 07″ E) (Fig. 1A). On 23 May 2018, 4 floating bags made of transparent polyethylene (volume of 11 m^3, 5 m deep and 2 m wide) were filled with surrounding fjord water from a depth of ~5 m. Mesocosm bags are permeable to 90% of photosynthetically active radiation (Vincent et al. 2023), but have no fluid exchange with the fjord water outside. Circulation within the 5 m deep mesocosm bags was maintained using airlift pumps (Castberg et al. 2001) throughout the experiment. Nutrients were added to mesocosm bags initially at a 16:1 ratio of nitrate to phosphate (1.6 µM nitrate as $NaNO_3$ and 0.1 µM phosphate as K_2PO_4). The addition of nutrients occurred at ~12:00 h local time daily on Days 0–7. Additions were then adjusted based on nutrient concentrations, with final nutrient addition concentrations being 20.8 µM nitrate and 1 µM phosphate. The experiment ran for a total of 22 d, reported as Day 1 until Day 22.

2.2. Paired dilution experiments

To estimate rates of phytoplankton growth, microzooplankton grazing and viral lysis, we used the paired dilution method (Landry & Hassett 1982, Landry et al. 1995, Evans et al. 2003). Dilution experiments were conducted every 2 to 3 d from Days 1 to 12, and daily from Days 12 to 22 to capture high-resolution changes in rates during the *Emiliania huxleyi* bloom. Dilution experiments were set up as described in Vincent et al. (2023); briefly, we used one high dilution level (20%) and an undiluted treatment (Morison & Menden-Deuer 2015, 2017). Water was collected at ~1 m depth and screened through a 200 µm mesh to remove larger mesozooplankton. Diluent was produced by gravity filtering whole seawater (WSW) through a 0.45 µm filter (PALL Acropak™ Membrane capsule), and for virus-free water through a tangential flow filter (TFF) of 100 kDa. To make sure experiments could be set up as rapidly as possible but still have similar chemical composition, TFF water was produced 1–2 d before experiments. Nutrients (10 µM nitrate and 1 µM phosphate) were only added to additional triplicate 100% WSW bottles since nutrients were added during the mesocosm experiment. All bottles were incubated for 24 h in an outdoor tank with continuous flow-through of ambient seawater to provide gentle agitation, and a screen to recreate light conditions within the upper 1 m of mesocosm bags.

2.3. Chlorophyll and flow cytometry measurements

Chlorophyll *a* (chl *a*) and flow cytometry were subsampled at an initial timepoint (T0) and after 24 h incubation (T24) for all dilution experiments. For chl *a*, 100–150 ml of seawater was filtered under low vacuum pressure through 47 mm Whatman GF/F filters, and extracted in the dark for 12 h in 7 ml of 97% methanol at 4°C. Fluorescence readings were conducted on a Turner TD700 fluorometer (Jespersen & Christoffersen 1987). Methanol blanks were included, and samples were read before and after a drop of 10% hydrochloric acid was added to correct for phaeophytin (Holm-Hansen & Riemann 1978).

For the determination of phytoplankton abundances from WSW and all diluted (20% WSW) bottles, flow cytometry samples were taken at T0 and T24 as in Vincent et al. (2023). Briefly, samples were fixed using 25% glutaraldehyde (final concentration <1%), inverted and then incubated at 4°C for up to 2 h, flash frozen in liquid nitrogen and finally stored at −80°C until analysis. Four phytoplankton groups were differentiated using a FACSCalibur (BD Biosciences), with a high flow rate (104–108 µl min^{-1}). Picoeukaryotes and nanoeukaryotes were differentiated based on red and orange fluorescence and side scatter, with *E. huxleyi* displaying enhanced side scatter due to the presence of extracellular coccoliths. Identification of *Synechococcus* was based on the presence of orange fluorescence (Larsen et al. 2004, Paulino et al. 2008, Mayers et al. 2020). Due to mislabelling of flow cytometry samples on Days 20 and 21, the samples from these dates were pooled as one experiment and are labelled as Day 20.5.

The apparent growth rates (k) of the total phytoplankton community (based on chl *a*) and flow cytometry phytoplankton groups were calculated as:

$$k = 1 / t \ln(C_t - C_0) \quad (1)$$

where t is the incubation time in days, and C_t and C_0 are the final and initial concentrations, respectively, of chl *a* or cell counts.

Mortality rates (g) were calculated as:

$$g = (k_d - k_1) / (1 - x) \quad (2)$$

where k_1 is the growth rate in 100% WSW with nutrient addition, k_d is the growth rate in the diluted treatment (20%), and x is the fraction of WSW. The intrinsic growth rate (μ) was calculated using k_2, which is the average growth rate without nutrients added:

$$\mu = g + k_2 \quad (3)$$

Significant differences (here, $p < 0.1$ due to high natural variability) were determined using paired t-tests between 100% WSW bottles with and without nutrients. If significant differences were seen, growth rates were calculated as above; if not significantly different, they were pooled for calculations. Grazing rates were also determined to be significant through paired t-tests between 100% WSW and diluted treatments. This was also conducted for viral lysis when observed, between diluted treatments with FSW and TFF water. If viral lysis was detected, intrinsic growth rates were calculated using both grazing and viral lysis rates ($g + v$).

Mortality rates that were negative were set to 0. For each group, the number of mortality rates set to 0 this way was: chl *a*, 34%, $n = 11$; picoeukaryotes, 41%, $n = 13$; *Synechococcus*, 41%, $n = 13$; nanoeukaryotes, 28%, $n = 9$; and *E. huxleyi*, 44%, $n = 14$.

Cell abundances from flow cytometry were converted to organic carbon using literature values from North Atlantic communities (Tarran et al. 2006) and cultures of *E. huxleyi* (Harvey et al. 2015) accounting for only the organic component of coccolithophore cells. The values used were: picoeukaryotes, 36.37 fmol C cell^{-1}; *Synechococcus*, 8.58 fmol C cell^{-1}; nanoeukaryotes, 0.76 pmol C cell^{-1}; and *E. huxleyi*, 0.68 pmol C cell^{-1}. To determine the concentration of carbon lost due to microzooplankton grazing or viral lysis, the T0 abundance (as determined by flow cytometry) of each group was converted into organic carbon and then multiplied by the mortality rate (grazing and/or viral lysis) to determine pmol C d^{-1} lost due to each process. This was only done for mortality rates that were determined to be significant. This calculation assumed no growth from the T0 population density and is therefore likely an underestimated value, but provides an indication of carbon flow due to mortality processes throughout the mesocosm experiment.

2.4. Molecular detection of phytoplankton taxa

To quantify the abundances of 2 specific phytoplankton populations (*E. huxleyi* and *Micromonas* spp.) in different size fractions, we collected samples for molecular analysis of the 2 target species as well as their specific viruses (*Emiliania huxleyi* virus [EhV] and *Micromonas pusilla* virus [MpV]). Water was collected as above for dilution experiments and siphoned into six 3 l polyethylene bottles, of which 3 were immediately used for filtration (T0), and 3 were incubated for 24 h in the outdoor tank used for dilution experiments without nutrient addition (T24). All equipment used for filtration was first washed with 10% HCl, followed by 3 washes in Milli-Q. The bench space was cleaned with a bleach solution to avoid contamination. At T0 and T24, 3 l of water was first passed through a 20 μm MilliPore Nylon filter with the filtrate collected. The 20 μm filter was rinsed 3 times with TFF (100 kDa) filtered water to remove any phytoplankton cells which had adhered to the filter or were loosely bound to larger organisms and/or particles; we termed this the predator size fraction. To provide a background quantification of the target organism(s) within the water sample, and detect cell-associated viral particles, 200–500 ml of the remaining filtrate was filtered through a 0.6 μm Whatman polycarbonate filter (Fig. 1B), which we termed the prey size fraction. After filtration, the filters were immediately placed into 1.5 ml Eppendorf tubes, with 360 μl of ATL buffer (QIAGEN) and 40 μl of Proteinase K, ensuring the filter was completely covered. The tubes were then left in a heat block set to 56°C overnight, before being transferred to a −20°C freezer until DNA extraction.

Eppendorf tubes containing filters were heated at 56°C for ~10 min prior to DNA extraction. Tubes containing filters were vortexed, spun down and then the filters were carefully removed using sterile pipette tips. All samples were extracted using the DNeasy Blood & Tissue kit (QIAGEN) according to the manufacturer's protocol, and eluted DNA was stored at −20°C until analysis. Quantification of phytoplankton and viruses was done using ddPCR (Bio-Rad Laboratories). ddPCR reactions were run with a total volume of 20 μl on a DX200 instrument (Bio-Rad Laboratories) using 5 μl of template DNA, 1× EvaGreen supermix (Bio-Rad Laboratories) and 250 nM (final concentration) of primers targeting a region of the 18S for *E. huxleyi* (Nejstgaard et al. 2008) and *Micromonas* spp. (Zhu et al. 2005), as well as the major capsid protein in EhV (Pagarete et al. 2009, Mayers et al. 2021) and MpV (present study) (Table S1 in the Supplement at www.int-res.com/articles/suppl/a090p141_supp.pdf) and

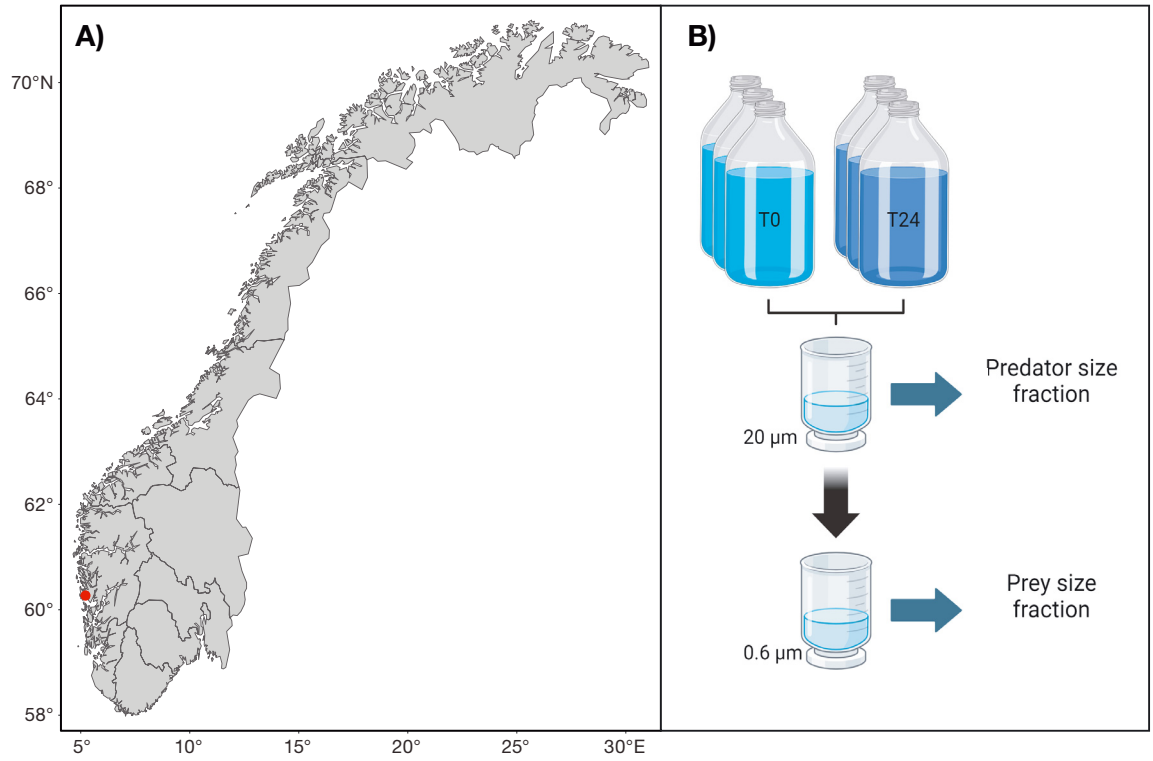

Fig. 1. (A) Location of Espegrend marine biological station (red dot) within Norway, and (B) overview of methodology for molecular detection of organisms and viruses. Triplicate bottles at T0 or after 24 h incubation (T24) were first filtered through 20 µm filters (predator size fraction) and then through 0.6 µm for the prey size fractions. ddPCR targeting algae was conducted on both size fractions, and for viruses only from the prey size fraction. Panel (B) was created in BioRender (K. Mayers, BioRender.com/q70d291)

ultra-pure water. Primers for MpV were designed, cloned, sequenced and blasted against the NCBI database (Text S1); this included a sample from Day 18 of the mesocosm experiment. They were also tested for specificity against other common algal viruses (Fig. S1). Complete PCR reactions were emulsified with QX200 Droplet Generation Oil for EvaGreen using the QX200 Droplet Generator, then transferred to a ddPCR 96-well plate. The PCR reaction was performed using these plates in a C1000 Touch thermocycler with deep-well module (Bio-Rad Laboratories) using the following settings: 95°C for 5 min, 40 cycles of 95°C for 30 s then 60°C (*E. huxleyi*), 61.4°C (*Micromonas* spp.), 64.7°C (EhV) or 60.1°C (MpV) for 1 min, 4°C for 5 min, 90°C for 10 min and finally an infinite hold at 4°C. Plates were equilibrated to room temperature for at least 10 min before analysis using the QX200 Droplet Reader (Bio-Rad Laboratories). Thresholds for positive/negative droplets were manually set using positive (algae or virus cultures) and negative (ultra-pure water) controls. To determine significant increases or decreases in copy number over 24 h, we used one-way ANOVAs assigning significance at $p \leq 0.1$ using the vegan package in R (Oksanen et al. 2022).

3. RESULTS

3.1. Development of mesocosm blooms

From an initial value of 2.2 ± 0.1 mg m^{-3}, chl *a* increased to 9.1 ± 0.9 mg m^{-3} on Day 10, before declining to 4.9 ± 0.2 mg m^{-3} on Day 12 (Fig. 2). A second peak (Day 18) reached a maximum concentration of 19.4 ± 0.9 mg m^{-3}. Picoeukaryote abundance increased rapidly from initial concentrations of 1.4 × 10^4 cells ml^{-1} to 9.7 × 10^4 cells ml^{-1} at Day 10 (Fig. 3A). Abundances continued to decline to 1.6 × 10^4 cells ml^{-1}, before a second increase at Day 20 (3.8 × 10^4 cells ml^{-1}). Abundances of *Synechococcus* were low at the beginning of the experiment (3.7 × 10^3 ml^{-1}) and remained low until Day 10, after which they fluctuated between 2.8 × 10^4 cells ml^{-1} (Day 19) and 8.3 × 10^3 cells ml^{-1} (Day 15) (Fig. 3B).

Nanoeukaryotes (except *Emiliania huxleyi*) showed rapid growth at the beginning of the experiment, and throughout the experiment displayed 3 peaks at Day 8 (1.9 × 10^4 cells ml^{-1}), Day 17 (1.4 × 10^4 cells ml^{-1}) and Day 20 (1.2 × 10^4 cells ml^{-1}) (Fig. 3C). The main peak of the coccolithophore *E. huxleyi* occurred at

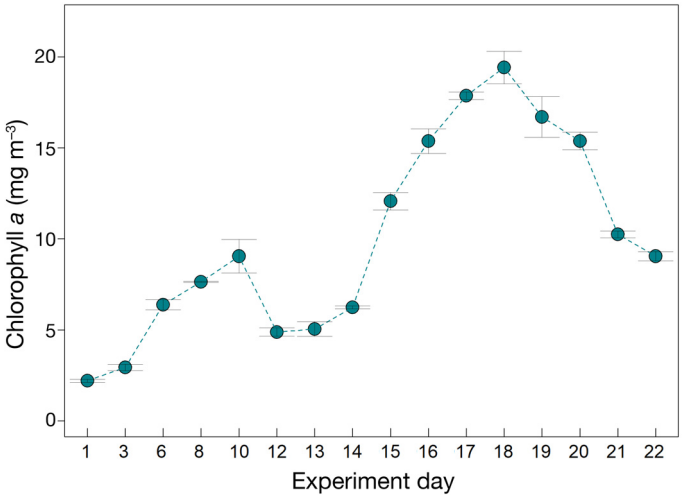

Fig. 2. Development of chlorophyll *a* throughout the mesocosm experiment. Error bars represent mean ± SD

Day 18 (1.1×10^5 cells ml^{-1}) from initial concentrations <100 cells ml^{-1} (Fig. 3D). From Day 8, the coccolithophore abundance was defined as a bloom (>1×10^3 cells ml^{-1}; Tyrrell & Merico 2004), and after the peak of *E. huxleyi* abundances on Day 18 they declined until the end of the experiment on Day 22.

3.2. Rates of mortality throughout the bloom

Mortality rates of the total phytoplankton community (chl *a*) were mostly dominated by microzooplankton grazing, with one incidence of significant viral lysis detected on Day 16 (0.3 ± 0.1 d^{-1}, p = 0.01) (Fig. 4A). In the beginning of the experiment, microzooplankton grazing rates varied from 0.3 to 0.4 d^{-1}, with a decline to undetectable on Day 8. Grazing rates were variable for the rest of the experiment, between undetectable and 0.4 d^{-1} including Day 16 (0.1 ±

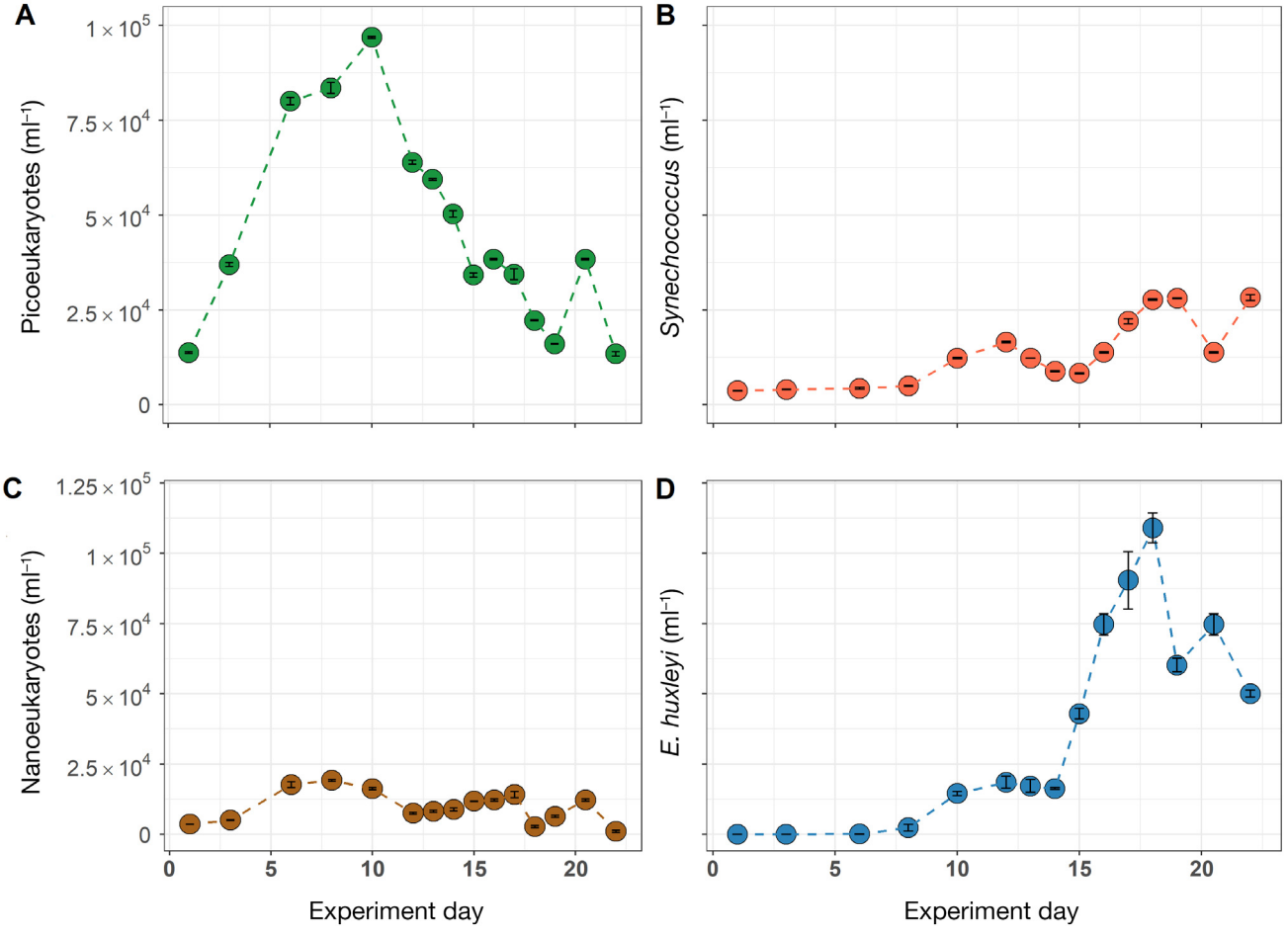

Fig. 3. Abundance of phytoplankton groups identified by flow cytometry. (A) Picoeukaryotes, (B) *Synechococcus*, (C) nanoeukaryotes and (D) *Emiliania huxleyi*. Error bars represent mean ± SD

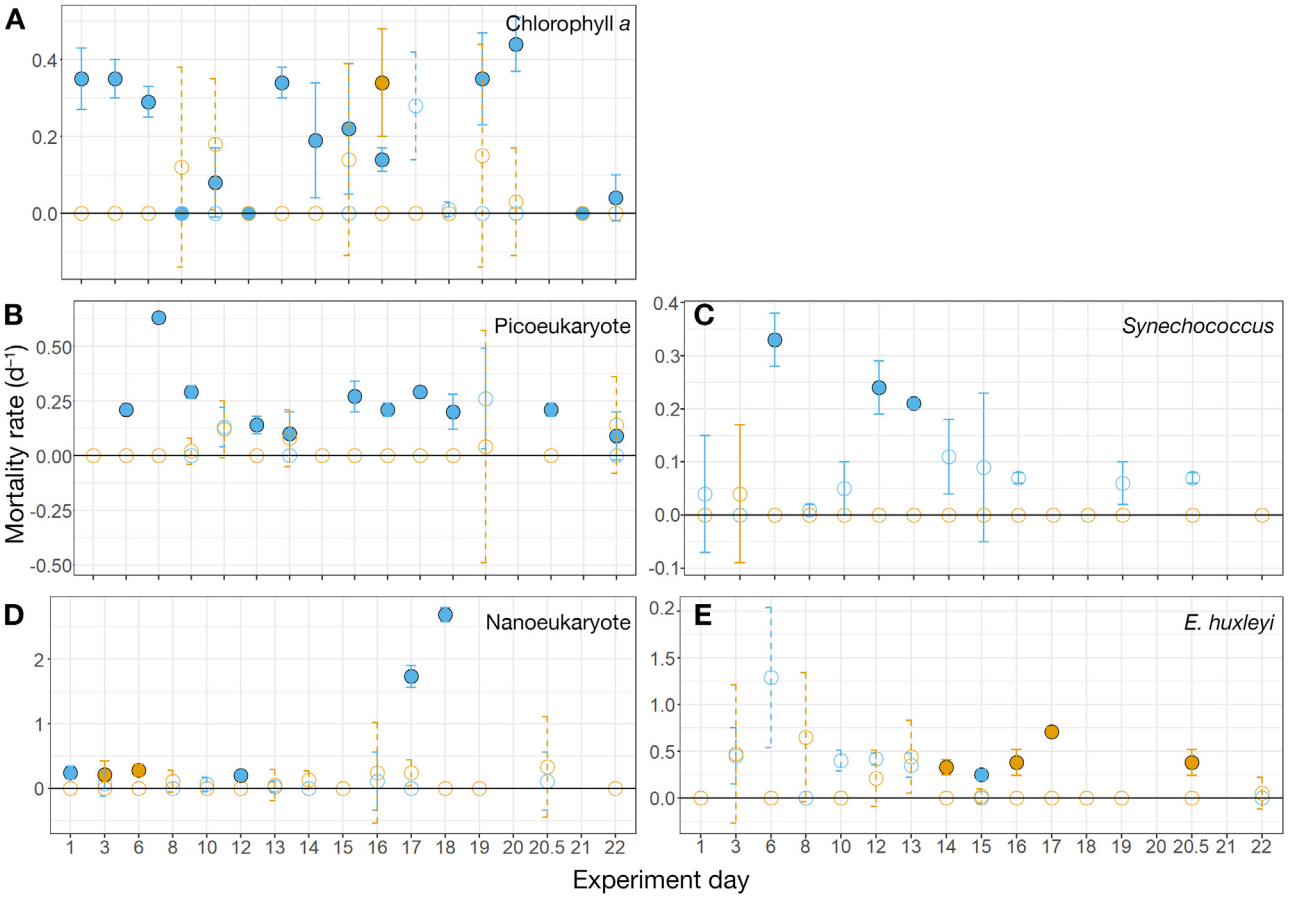

Fig. 4. Mortality rates of microzooplankton grazing (blue) and viral lysis (orange) for (A) chlorophyll *a*, (B) picoeukaryotes, (C) *Synechococcus*, (D) nanoeukaryotes and (E) *Emiliania huxleyi*. Filled circles are significant ($p < 0.1$) rates and non-filled are non-significant rates or those set to zero. Samples on Days 20 and 21 were pooled and displayed as Day 20.5. Error bars are mean ± SD and are shown with solid lines for significant rates and dashed lines for non-significant rates

0.0 d^{-1}), when viral lysis was also significant (0.3 ± 0.1 d^{-1}, $p = 0.01$).

We did not observe any significant viral lysis at any time of the mesocosm experiment for the picoplankton groups, picoeukaryotes and *Synechococcus* (Fig. 4B,C). Significant microzooplankton grazing was observed on 11 experimental days for picoeukaryotes and 3 for *Synechococcus*, varying between 0.1 ± 0.1 and 0.6 ± 0.0 d^{-1} and 0.2 ± 0.0 and 0.3 ± 0.1 d^{-1}, respectively. The highest grazing rates for both picoeukaryotes and *Synechococcus* were observed on Day 6.

Mortality rates on the nanoeukaryote population were initially dominated by microzooplankton grazing (0.2 ± 0.1 d^{-1}) with undetectable viral lysis (Fig. 4D). The importance of viral lysis increased on Day 3 (0.2 ± 0.2 d^{-1}) and Day 6 (0.3 ± 0.1 d^{-1}). After this, mortality rates remained undetectable, aside from microzooplankton grazing on Day 12 (0.2 ± 0.1 d^{-1}) and high grazing rates on Days 17 and 18 (1.7 ± 0.2 and 2.7 ± 0.1 d^{-1}, respectively). *E. huxleyi* mortality was dominated by viral lysis, varying between 0.3 ± 0.1 and 0.7 ± 0.0 d^{-1} (Fig. 4E). Significant microzooplankton grazing was only detected on Day 15 (0.3 ± 0.1 d^{-1}, $p = 0.04$).

3.3. Carbon flow through mortality pathways

For picoeukaryotes and *Synechococcus*, up to 100% of daily organic carbon production loss within these groups was being funnelled through microbial grazers (Table 1). For nanoeukaryotes, within the early phase of the experiment, when they appeared to dominate the carbon biomass (Fig. S2), most carbon losses were due to viral lysis (Table 1), particularly on Days 3 and 6. Losses due to microzooplankton predation were considerable on Days 17 and 18. Throughout the whole experiment, on average the losses to microzooplank-

Table 1. Loss of organic carbon calculated from microzooplankton grazing or viral lysis for different phytoplankton groups determined by flow cytometry. Values are calculated using carbon conversion factors of initial counts (T0) from dilution experiments and multiplying by grazing or viral lysis rates from dilution experiments

Experiment day	Carbon loss (nmol C)							
	Picoeukaryote		*Synechococcus*		Nanoeukaryote		*Emiliania huxleyi*	
	Grazing	Virus	Grazing	Virus	Grazing	Virus	Grazing	Virus
1					0.65			
3	0.28					0.80		
6	1.85		0.01			3.76		
8	0.90							
10								
12	0.33		0.03		1.13			
13	0.21		0.02					
14								3.66
15	0.34						7.17	
16	0.29							19.37
17	0.37				18.61			43.65
18	0.16				5.65			
19								
20	0.29							19.37
22	0.04							
Sum of losses	5.06	0	0.06	0	26.04	4.56	7.17	86.05
Percentage	100	0	100	0	85	15	8	92

ton grazing and viral lysis represented 85.1 and 14.9%, respectively, of nanoeukaryote carbon.

The coccolithophore *E. huxleyi* showed losses due to microzooplankton grazing only on Day 15, and viral lysis on 5 occasions (Table 1). Mortality losses, particularly on Day 17, were during periods of high *E. huxleyi* biomass, which led to significant carbon losses due to viral infection. On average, over the whole experiment, organic carbon losses due to microzooplankton grazing and viral lysis were 6.4 and 93.6%, respectively.

3.4. Molecular detection of predator–prey and viral interactions

The prasinophyte *Micromonas* spp. was detected in all samples analysed (Fig. 5A,B). The prey size fraction (0.6 µm) displayed an order of magnitude greater copy numbers than in the predator size fraction (20 µm) (0.6×10^3 to 1.5×10^5 and 1 to 86 gene copies ml^{-1}, respectively). For both size fractions, the highest T0 copy number was observed on Day 6, suggesting that the increase in picoeukaryotes (Fig. 3B) coincides with an increase in *Micromonas* spp. During 4 experiments (Days 3, 6, 10 and 18), we observed statistically significant ($p \leq 0.1$) increases in copy numbers from T0 to T24 in the predator size fraction (Fig. 5A). For all these dates, aside from Day 10, we also observed significant microzooplankton grazing (Fig. 4B). On Days 6 and 10, this was accompanied by a significant decrease in the prey size fraction ($p < 0.05$; Fig. 5B), which was also observed on Days 14 and 20 ($p < 0.02$). MpV within the prey size fraction was detected throughout the experiment (Fig. 5C), with a peak around Day 10, which coincided with the picoeukaryote decline. Viral lysis was detected for picoeukaryotes on Days 8 and 10; however, this was determined to be non-significant (Table S2). MpV abundances declined following this date, with a slight significant increase ($p < 0.02$) on Day 16 over 24 h. No viral lysis on picoeukaryotes was observed on this date; however, for chl *a* it was (Fig. 4A).

ddPCR analysis targeting *E. huxleyi* within the predator (>20 µm) size fraction also displayed detection throughout the entire mesocosm experiment (Fig. 6A). Between T0 and T24, only the experiments conducted on Days 6, 8, 10, 16 and 18 determined significantly higher detections after incubations ($p < 0.07$). Although grazing was observed on Days 6 and 10 (Table S2), these were non-significant from dilution experiments.

Within the prey fraction, *E. huxleyi* was also detected at all times sampled (Fig. 6B). Statistically significant differences between T0 and T24 were observed for Days 3, 10, 12, 18 and 20 ($p < 0.1$). For all dates aside from Day 20, the difference was an increase in copy numbers, particularly for Days 3 and 12, where both dates also showed slightly positive net growth rates (Fig. S3D). The decline at Day 20 coin-

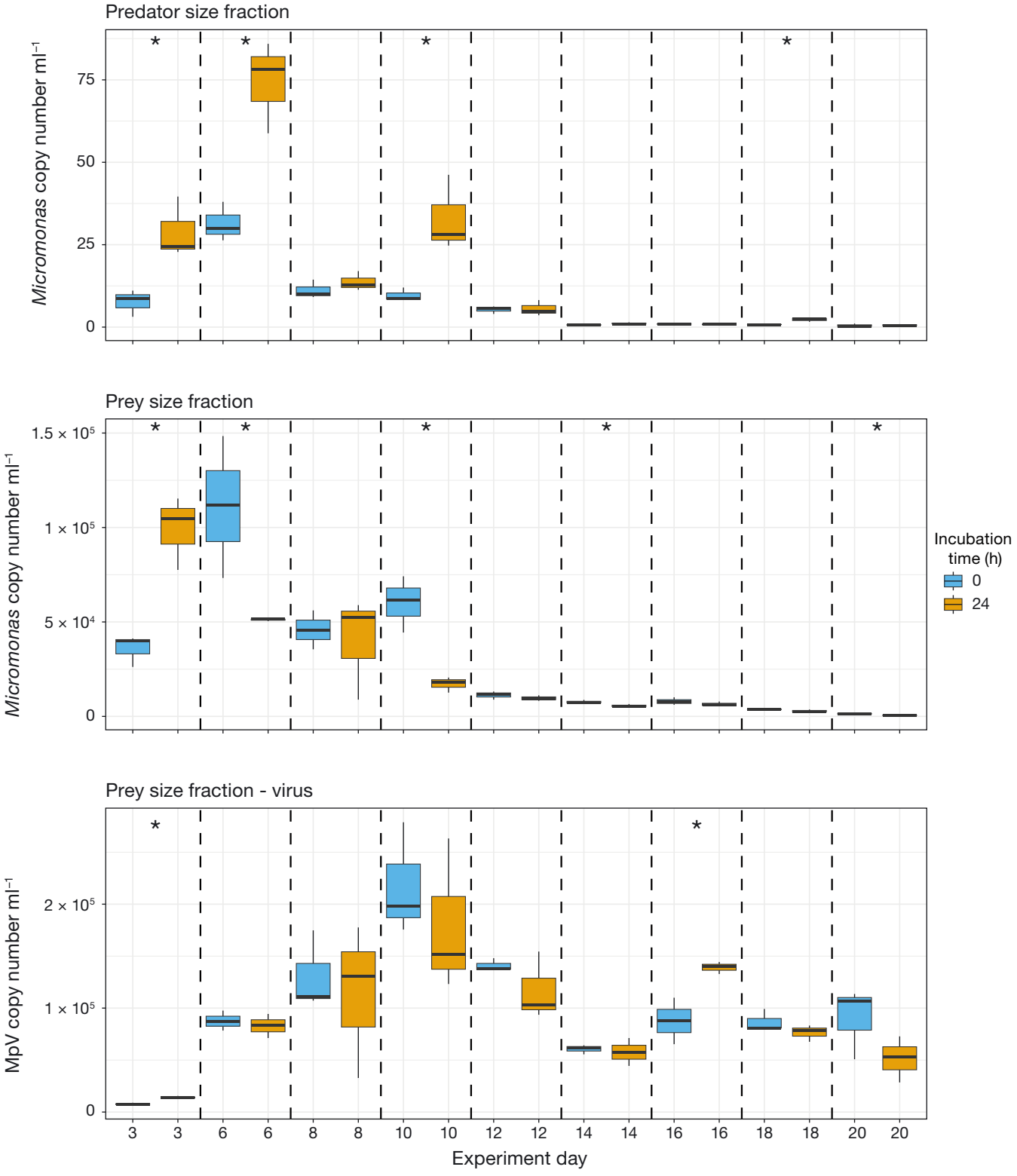

Fig. 5. Copy numbers from ddPCR of *Micromonas* spp. within the (A) 20 µm predator size fraction and (B) 0.6 µm prey size fraction, and (C) *Micromonas pusilla* virus (MpV) within the 0.6 µm prey size fraction during experiments conducted throughout the mesocosm. * Significant difference between T0 and T24 ($p < 0.1$) determined by one-way ANOVA. Boxes indicate the 25th and 75th percentile with median values displayed with a bold line. Whiskers show the minimum and maximum values

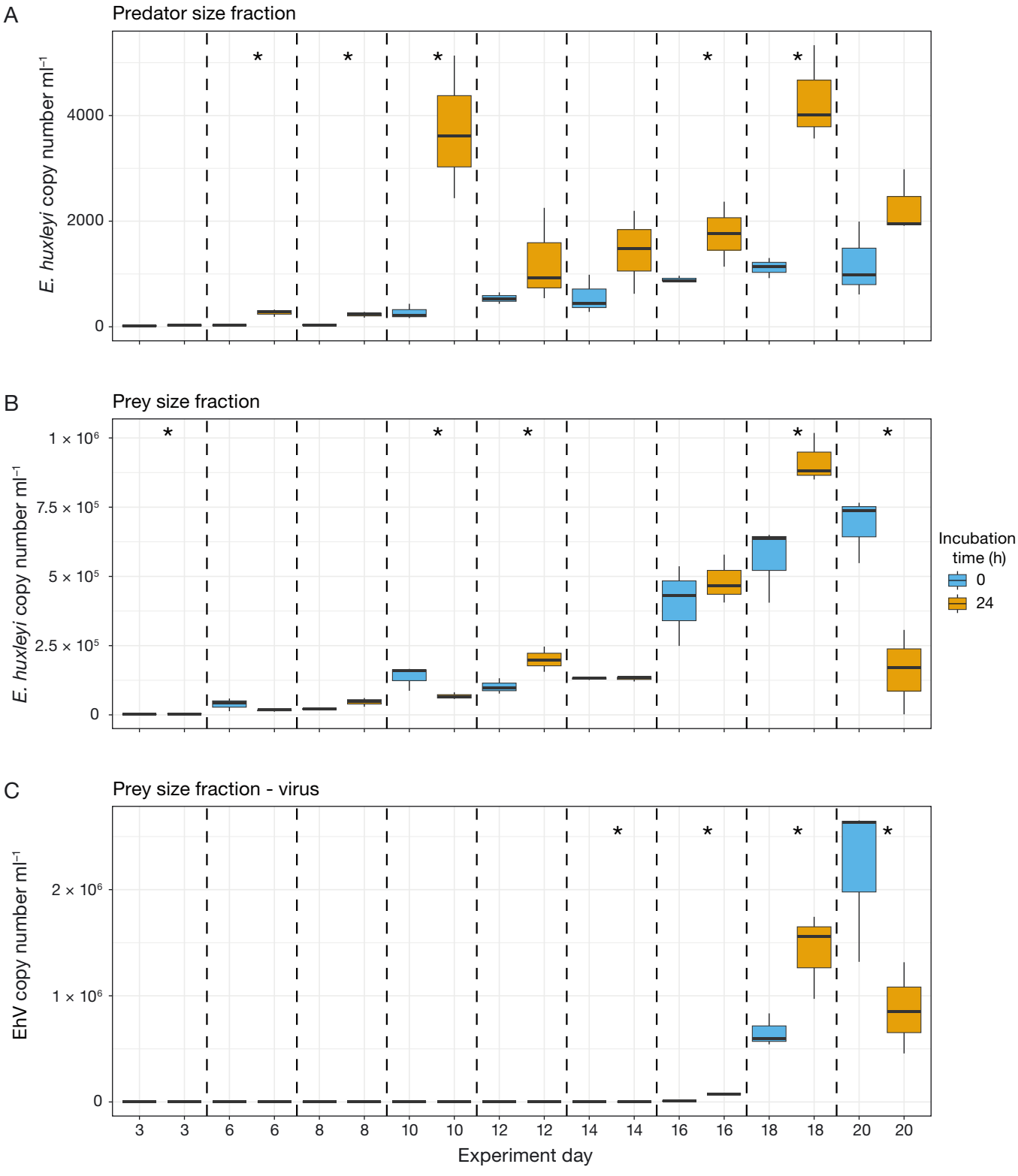

Fig. 6. Copy numbers from ddPCR of *Emiliania huxleyi* within the (A) 20 µm predator size fraction and (B) 0.6 µm prey size fraction, and (C) *Emiliania huxleyi* virus (EhV) within the 0.6 µm prey size fraction during experiments conducted throughout the mesocosm. * Significant difference between T0 and T24 ($p < 0.1$) determined by one-way ANOVA. Boxes indicate the 25th and 75th percentile with median values displayed with a bold line. Whiskers show the minimum and maximum values

cides with that observed by flow cytometry (Fig. 3C). The T0 abundance of *E. huxleyi* continued to increase throughout the entire experiment, reaching a maximum on Day 20 ($6.8 \times 10^5 \pm 1.2 \times 10^5$ copies ml^{-1}).

Detection of EhV within the prey size fraction (0.6 µm) was undetectable until Day 12 of the experiment (Fig. 6C). Following this date there was a gradual increase in abundance, including statistically significant increases between 24 h incubations on Days 14, 16 and 18 ($p < 0.1$). Significant viral lysis of *E. huxleyi* was observed on Days 14, 16 and 17 (Fig. 4E).

4. DISCUSSION

In this study, we show that mortality rates due to microzooplankton predation and viral lysis can shift rapidly within phytoplankton communities, particularly within individual groups. The smaller phytoplankton (picoeukaryotes, *Synechococcus*) appear to succumb to microzooplankton grazing rather than viral lysis, whereas nanoeukaryotes and *Emiliania huxleyi* both displayed demise due to viral lysis. Our data indicate that one mortality process dominates in phytoplankton groups at certain times. During these high biomass scenarios, more carbon is funnelled through viral-mediated pathways rather than microzooplankton-mediated food webs.

4.1. Microzooplankton grazing versus viral lysis

Our study results indicate that either microzooplankton- or viral-mediated mortality dominates at any given time, with only one instance of significant occurrence for both processes being detected (chl *a* on Day 16). This pattern aligns with findings both from weekly sampling in a subtropical estuary in Georgia, USA, and experiments in the California Current Ecosystem, where simultaneous significant grazing and viral lysis events were infrequent (Pasulka et al. 2015, Anderson & Harvey 2019). In the Southern Ocean, seasonal variability was observed between microzooplankton grazing and viral lysis on different phytoplankton groups, with high lysis rates coinciding with low grazing rates and vice versa (Biggs et al. 2021). These findings suggest that our results reflect a general phenomenon observed across broad phytoplankton groups identified using flow cytometry.

Paired dilution experiments are one of the only available techniques which provide simultaneous rate measurements of microzooplankton predation and viral lysis. A significant portion of our results provided either negative or non-significant results. Many processes can lead to this, including trophic cascades within dilution bottles mediated through the removal of larger (>200 µm) zooplankton (Calbet & Saiz 2013), mixotrophy (Duarte Ferreira et al. 2021) and the release of dissolved organic matter through the filtration process (Pree et al. 2016), leading to stimulated growth of organisms. At low abundances (e.g. *E. huxleyi* during the early bloom stage) it can be difficult with flow cytometry to determine accurate cell numbers, leading to high variability in calculated rates. Combining flow cytometry with methods able to handle low abundances (e.g. ddPCR) could lead to better understanding of dynamics during pre- and post-bloom periods.

Mortality of picoeukaryotes and *Synechococcus* was only due to microzooplankton grazing during this study. Following the decline of the first bloom, the abundance of *Synechococcus* increased in parallel with microzooplankton grazing rates on this group, likely leading to their subsequent decline. A meta-analysis of dilution data, including those presented here, indicated reduced microzooplankton predation pressure on *Synechococcus* compared to picoeukaryotes, nanoeukaryotes or *E. huxleyi* (Mayers et al. 2020). Our data suggest that certain strains of *Synechococcus* may be more susceptible to grazing pressure than others, as observed in laboratory settings (Zwirglmaier et al. 2009), and in natural environments, a high selectivity by grazer assemblages on *Synechococcus* and other picoplankton was observed (Landry et al. 2023). Predator community composition may also play a role, as both picoplankton groups exhibited the highest rates of microzooplankton grazing on the same date (Day 6). During this early bloom stage, mixotrophic and heterotrophic grazers appeared to dominate the eukaryotic plankton fraction, whilst ciliate abundance was low and increased throughout the mesocosm experiment (Vincent et al. 2023).

In a different mesocosm experiment focusing on picoeukaryotes, grazing was also identified as the dominant mortality process during a 3 d bloom (Evans et al. 2003). However, contrary to our findings, viral lysis was a significant mortality process for picoeukaryotes, with comparable magnitudes to grazing rates in one experiment (0.29 and 0.30 d^{-1} for viral lysis and grazing, respectively). Although viral lysis rates were observed in our experiment for picoeukaryotes (Day 10, 0.12 d^{-1}), they were not statistically significant (Table S2). Detection of MpV by ddPCR also indicated a significant increase on this date, suggesting that viral lysis rates might not have been detected due to the coarse groupings (i.e. pico-

eukaryotes) used in the modified dilution technique. If some picoeukaryote organisms did succumb to viral infection, but others did not, or were growing or grazed in the same experiment, this would obscure detection of the rate measurements. Additionally, our 2 d sampling period during the highest picoeukaryote abundance may have missed the peak of viral mortality, highlighting the importance of frequent sampling during bloom events. The use of ddPCR on a 0.6 µm filter allows measurement of viral production within the cell, rather than specifically lysis, as many algal viruses can pass through the filter (Chaudhari et al. 2021, Mayers et al. 2023). Nevertheless, our results support the observations of Evans et al. (2003) that microzooplankton grazing is the primary cause of picoeukaryote abundance decline, consistent with the sustained low abundance observed throughout our experiment.

Viral infection of *E. huxleyi* has been observed to increase (Evans & Wilson 2008) and decrease (Goode et al. 2019) grazing pressure relative to uninfected cells in laboratory experiments. Our data support the latter, as grazing was only significant on *E. huxleyi* on one day (Day 15), whilst viral lysis was observed in multiple experiments after this date, with grazing being non-significant. However, after Day 15, the abundance of *E. huxleyi* reached concentrations that have been shown to have a negative impact on the growth of predator populations (>5.5×10^4 cells ml^{-1}) (Harvey et al. 2015), hypothesised to be due to the calcium carbonate buffering food vacuoles. In mesocosm communities, ingestion of *E. huxleyi* is unaffected by calcification state when compared with nanoeukaryotes and picoeukaryotes (Mayers et al. 2020). However, it is worth noting that digestion inhibition could serve as a possible defence mechanism at high densities. Further analysis is required to understand how microzooplankton communities respond to such high concentrations of calcified *E. huxleyi*, as well as the interaction between viral infection and microzooplankton grazing in natural communities.

During the 2 observed blooms, nanoeukaryotes and *E. huxleyi* were the dominant phytoplankton groups in terms of carbon content, as determined by flow cytometry. These 2 groups were also the only ones that exhibited significant viral lysis rates. Although picoeukaryotes dominated numerically, we did not observe significant viral lysis on this group (Table S2), which may be due to the limitations of the dilution method or due to the high diversity of organisms within the groupings provided by flow cytometry (Marie et al. 2010). Through metabarcoding of global marine eukaryotes, a 'pico-nano' size fraction (0.8–5 µm) showed higher diversity than the 'nano' size fraction (5–20 µm) (de Vargas et al. 2015). In our study, it is possible that the nanoeukaryotes were dominated by fewer species, leading to detection of viral lysis, whilst for picoeukaryotes this was obscured due to greater within-group diversity. Viral lysis can also impact the diversity of other organisms within marine phytoplankton groups (Thingstad 2000). In our mesocosm experiment, the 18S diversity of nanoplankton (2–20 µm) displayed greater divergence from initial conditions in highly infected mesocosms, particularly after bloom decline (Vincent et al. 2023). Although we did not determine the molecular diversity of *E. huxleyi*, the increase in diversity appears to operate on similar-sized phytoplankton groups.

Within *E. huxleyi* blooms it is generally accepted that viruses lead to their termination (Bratbak et al. 1993, Wilson et al. 2002, Vardi et al. 2012). However, various experiments in shelf sea regions have demonstrated high grazing (up to 79% of *E. huxleyi* production) during bloom events (Holligan et al. 1993, Mayers et al. 2019). Within our study, significant grazing was detected only during bloom formation, with viral lysis being the most probable cause of bloom demise. The density within this mesocosm experiment is much higher than in typical *E. huxleyi* coastal or open-ocean blooms (2000–3000 cells ml^{-1}; Poulton et al. 2013); however, such high abundances are typical of *E. huxleyi* blooms within fjord environments (Tyrrell & Merico 2004). Such high densities could have led to enhanced viral infection through density-driven means, leading to more susceptible cells encountering infectious virus particles. These same densities may have led to reduced predation due to digestion inhibition (Harvey et al. 2015) as discussed above, and supported by the negative correlation between EhV and ciliates measured in this experiment (Vincent et al. 2023).

4.2. Molecular dynamics of *E. huxleyi* and *Micromonas* spp. during the mesocosm experiment

Flow cytometry provides valuable information on the dynamics of broad phytoplankton groups based on size or other morphological characteristics. However, to directly investigate specific taxa of interest, molecular tools become essential. For instance, molecular analysis using *Micromonas*-specific primers revealed instances where growth rates estimated from dilution experiments and molecular incubations were similar (Fig. S3A). An intriguing observation on Day 8

was a decline in *Micromonas* spp. copy numbers in prey water fractions compared to Day 6, despite the continued increase in picoeukaryotes according to flow cytometry data. This discrepancy could be attributed to another picoeukaryote contributing to the increase in FCM abundance and the grazing observed on that date. One possible candidate is *Bathyococcus*, which was observed during this mesocosm experiment and has been found in subpolar Atlantic waters during spring (Bolaños et al. 2020, Vincent et al. 2023). Enhancing the resolution of dynamics on phytoplankton groups such as picoeukaryotes and nanoeukaryotes cannot be fully resolved with flow cytometry, but may be achieved through the further development of molecular grazing methods, such as incorporating multiplexing of multiple PCR targets akin to fluorescence *in situ* hybridization methods (Fuchs et al. 2005), particularly considering the complexity of these groups (Marie et al. 2010, de Vargas et al. 2015).

Several coccolithophores, including *E. huxleyi*, are known to have both a diploid calcified form and a naked haploid form (Cros et al. 2000). In *E. huxleyi*, viral infection can induce a shift to naked diploid or haploid forms (Frada et al. 2008, 2017), during which the cells become resistant to viral infection or (at the very least) to lysis, while still expressing viral transcripts (Mordecai et al. 2017). Coinciding with the decline in *E. huxleyi* cells (Days 18 to 19), we also noticed an increase in the nanoeukaryote population, potentially comprising naked or haploid *E. huxleyi* cells. Molecular incubation experiments on Day 18 showed a significant increase in *E. huxleyi* copy numbers in the 0.6 µm size fraction, as well as T0 on Day 20 compared to T0 at Day 18, supporting the occurrence of this switch within the mesocosm experiment. On Days 17 and 18, the highest rates of microzooplankton grazing on nanoeukaryote populations were observed, further confirmed by significant enhancement in the copy number of *E. huxleyi* identified in the predator size fraction during molecular incubation experiments on these dates. Grazing rates on cultured naked and calcified *E. huxleyi* have been found to be strain-specific rather than related to degree of calcification (Harvey et al. 2015). However, it is plausible that haploid cells are more palatable to the grazer community at this time compared with calcified cells due to a variety of strain-specific chemical or biological factors, rather than a loss of the calcium carbonate exoskeleton.

Detection within the predator size fraction (>20 µm) demonstrated significant increases during incubations for both organisms. In the case of *Micromonas* spp., this coincided with significant grazing rates from dilution experiments on several occasions. However, this was not the case for *E. huxleyi*. A significant increase in *E. huxleyi* copy numbers within the predator size fraction was noted, coinciding with elevated predation rates on nanoeukaryotes towards the end of the experiment. This observation further supports the hypothesis that the nanoeukaryotes encompass naked diploid or haploid *E. huxleyi* forms susceptible to ingestion. It is noteworthy that microzooplankton typically maintain highly acidic food vacuoles (pH ~3–5) (Nagata & Kirchman 1992, Gonzalez et al. 1993) and exhibit rapid digestion times (75–120 min; Capriulo & Degnan 1991, Dolan & Šimek 1997), implying significant digestion of ingested prey DNA over 24 h. Frequent sampling over a shorter duration would provide a more accurate assessment of ingestion and digestion rates for various organisms applying ddPCR.

Significant enhancements in EhV copy numbers were detected on the same or similar dates as viral lysis was observed for *E. huxleyi* in dilution experiments (Fig. 4E), except for Day 20, when EhV copy numbers declined (Fig. 6C). Like MpV, this may be due to the release of viral particles from cell lysis, causing them to no longer be associated with the 0.6 µm size fraction. Future studies should include sampling of the water passing through the 0.6 µm filter to provide information on the number of free virus particles and cell lysis, enabling a better comparison with that measured by the paired-dilution technique (Staniewski & Short 2018). Our findings suggest that a combination of flow cytometry and quantitative molecular techniques holds promise for determining mortality processes on specific phytoplankton groups, shedding light on the intricate dynamics within marine microbial communities.

5. CONCLUSION

The fate of carbon within the pelagic food web differs greatly depending on whether phytoplankton are grazed or lysed by a virus. Determining the rates of different mortality processes on phytoplankton is important not just for their population dynamics but also to understand the biogeochemical implications of death. Using flow cytometry, we can estimate these rates on phytoplankton groups; however, to gain a deeper understanding of rates on specific taxa, we require the use of quantitative molecular tools. The first phytoplankton bloom, consisting mostly of picoeukaryotes and nanoeukaryotes, was terminated by a combination of microzooplankton grazing and viral

lysis on each group, respectively, with the second *Emiliania huxleyi* bloom being terminated by viral infection. This likely led to high recycling of carbon in the upper ocean by the viral shunt (Suttle 2005), or enhanced export of material due release of sticky colloidal material (e.g. TEP) and subsequent export of material (Vardi et al. 2012, Laber et al. 2018, Vincent et al. 2023). The relative balance of these processes will have major implications for carbon cycling on regional and global scales. Utilising these techniques will further enhance our understanding of the ecological and biogeochemical processes occurring within marine ecosystems.

Acknowledgements. We thank Assaf Vardi and all the team members of the AQUACOSM VIMS-Ehux project for setting up and conducting the mesocosm experiment, including the staff at Espegrend marine biological station. This research was supported by EU Horizon2020-INFRAIA project AQUACOSM (no. 731065), AQUACOSM-plus (no. 871081) and Norwegian Research Council project MIXsTRUCT (no. 280414). We also thank 2 anonymous reviewers for their helpful and constructive comments on an earlier version of the manuscript.

LITERATURE CITED

Anderson SR, Harvey EL (2019) Seasonal variability and drivers of microzooplankton grazing and phytoplankton growth in a subtropical estuary. Front Mar Sci 6:174

Balch WM, Bates NR, Lam PJ, Twining BS and others (2016) Factors regulating the Great Calcite Belt in the Southern Ocean and its biogeochemical significance. Global Biogeochem Cycles 30:1124–1144

Baudoux AC, Veldhuis MJW, Noordeloos AAM, Van Noort G, Brussaard CPD (2008) Estimates of virus- vs. grazing induced mortality of picophytoplankton in the North Sea during summer. Aquat Microb Ecol 52:69–82

Biggs TEG, Huisman J, Brussaard CPD (2021) Viral lysis modifies seasonal phytoplankton dynamics and carbon flow in the Southern Ocean. ISME J 15:3615–3622

Bolaños LM, Lee K, Choi CJ, Worden AZ and others (2020) Small phytoplankton dominate western North Atlantic biomass. ISME J 14:1663–1674

Bratbak G, Egge JK, Heldal M (1993) Viral mortality of the marine alga *Emiliania huxleyi* (Haptophyceae) and termination of algal blooms. Mar Ecol Prog Ser 93:39–48

Calbet A, Landry MR (2004) Phytoplankton growth, microzooplankton grazing, and carbon cycling in marine systems. Limnol Oceanogr 49:51–57

Calbet A, Saiz E (2005) The ciliate-copepod link in marine ecosystems. Aquat Microb Ecol 38:157–167

Calbet A, Saiz E (2013) Effects of trophic cascades in dilution grazing experiments: from artificial saturated feeding responses to positive slopes. J Plankton Res 35:1183–1191

Capriulo GM, Degnan C (1991) Effect of food concentration on digestion and vacuole passage time in the heterotrichous marine ciliate *Fibrea salina*. Mar Biol 110:199–202

Castberg T, Larsen A, Sandaa RA, Brussaard CPD and others (2001) Microbial population dynamics and diversity during a bloom of the marine coccolithophorid *Emiliania huxleyi* (Haptophyta). Mar Ecol Prog Ser 221:39–46

Chaudhari HV, Inamdar MM, Kondabagil K (2021) Scaling relation between genome length and particle size of viruses provides insights into viral life history. iScience 24:102452

Cros L, Kleijne A, Zeltner A, Billard C, Young JR (2000) New examples of holococcolith–heterococcolith combination coccospheres and their implications for coccolithophorid biology. Mar Micropaleontol 39:1–34

de Vargas C, Audic S, Henry N, Decelle J and others (2015) Eukaryotic plankton diversity in the sunlit ocean. Science 348:1261605–1/11

Demory D, Baudoux AC, Monier A, Simon N and others (2019) Picoeukaryotes of the *Micromonas* genus: sentinels of a warming ocean. ISME J 13:132–146

Dolan JR, Šimek K (1997) Processing of ingested matter in *Strombidium sulcatum*, a marine ciliate (Oligotrichida). Limnol Oceanogr 42:393–397

Duarte Ferreira G, Romano F, Medic N, Pitta P and others (2021) Mixoplankton interferences in dilution grazing experiments. Sci Rep 11:23849

Evans C, Wilson WH (2008) Preferential grazing of *Oxyrrhis marina* on virus-infected *Emiliania huxleyi*. Limnol Oceanogr 53:2035–2040

Evans C, Archer SD, Jacquet S, Wilson WH (2003) Direct estimates of the contribution of viral lysis and microzooplankton grazing to the decline of a *Micromonas* spp. population. Aquat Microb Ecol 30:207–219

Frada M, Probert I, Allen MJ, Wilson WH, de Vargas C (2008) The 'Cheshire Cat' escape strategy of the coccolithophore *Emiliania huxleyi* in response to viral infection. Proc Natl Acad Sci USA 105:15944–15949

Frada MJ, Rosenwasser S, Ben-Dor S, Shemi A, Sabanay H, Vardi A (2017) Morphological switch to a resistant subpopulation in response to viral infection in the bloom-forming coccolithophore *Emiliania huxleyi*. PLOS Pathog 13:e1006775

Fuchs BM, Woebken D, Zubkov MV, Burkill P, Amann R (2005) Molecular identification of picoplankton populations in contrasting waters of the Arabian Sea. Aquat Microb Ecol 39:145–157

Gonzalez JM, Iriberri J, Egea L, Barcina I (1990) Differential rates of digestion of bacteria by freshwater and marine phagotrophic protozoa. Appl Environ Microbiol 56: 1851–1857

Gonzalez JM, Sherr BF, Sherr EB (1993) Digestive enzyme activity as a quantitative measure of protistan grazing: the acid lysozyme assay for bacterivory. Mar Ecol Prog Ser 100:197–206

Goode AG, Fields DM, Archer SD, Martínez JM (2019) Physiological responses of *Oxyrrhis marina* to a diet of virally infected *Emiliania huxleyi*. PeerJ 7:e6722

Guidi L, Chaffon S, Bittner L, Eveillad D and others (2016) Plankton networks driving carbon export in the oligotrophic ocean. Nature 532:465

Harvey EL, Bidle KD, Johnson MD (2015) Consequences of strain variability and calcification in *Emiliania huxleyi* on microzooplankton grazing. J Plankton Res 37:1137–1148

Hindson BJ, Ness KD, Masquelier DA, Belgrader P and others (2011) High-throughput droplet digital PCR system for absolute quantitation of DNA copy number. Anal Chem 83:8604–8610

Holligan PM, Fernández E, Aiken J, Balch WM and others (1993) A biogeochemical study of the coccolithophore,

Emiliania huxleyi, in the North Atlantic. Global Biogeochem Cycles 7:879–900
Holm-Hansen O, Riemann B (1978) Chlorophyll a determination: improvements in methodology. Oikos 30:438–447
Howard-Varona C, Roux S, Bowen BP, Silva LP and others (2022) Protist impacts on marine cyanovirocell metabolism. ISME Commun 2:94
Hunter JE, Frada MJ, Fredricks HF, Vardi A, Van Mooy BAS (2015) Targeted and untargeted lipidomics of *Emiliania huxleyi* viral infection and life cycle phases highlights molecular biomarkers of infection, susceptibility, and ploidy. Front Mar Sci 2:81
Irigoien X, Flynn KJ, Harris RP (2005) Phytoplankton blooms: a 'loophole' in microzooplankton grazing impact? J Plankton Res 27:313–321
Jespersen AM, Christoffersen K (1987) Measurements of chlorophyll-a from phytoplankton using ethanol as extraction solvent. Arch Hydrobiol 109:445–454
Klaas C, Archer DE (2002) Association of sinking organic matter with various types of mineral ballast in the deep sea: implications for the rain ratio. Global Biogeochem Cycles 16:1–14
Kokkoris V, Vukicevich E, Richards A, Thomsen C, Hart MM (2021) Challenges using droplet digital PCR for environmental samples. Appl Microbiol 1:74–88
Laber CP, Hunter JE, Carvalho F, Collins JR and others (2018) Coccolithovirus facilitation of carbon export in the North Atlantic. Nat Microbiol 3:537–547
Landry MR, Hassett RP (1982) Estimating the grazing impact of marine micro-zooplankton. Mar Biol 67:283–288
Landry MR, Kirshtein J, Constantinou J (1995) A refined dilution technique for measuring the community grazing impact of microzooplankton, with experimental tests in the central equatorial Pacific. Mar Ecol Prog Ser 120: 53–63
Landry MR, Stukel MR, Selph KE, Goericke R (2023) Coexisting picoplankton experience different relative grazing pressures across an ocean productivity gradient. Proc Natl Acad Sci USA 120:e2220771120
Larsen A, Flaten GAF, Sandaa RA, Castberg T and others (2004) Spring phytoplankton bloom dynamics in Norwegian coastal waters: microbial community succession and diversity. Limnol Oceanogr 49:180–190
Lovejoy C, Vincent WF, Bonilla S, Roy S and others (2007) Distribution, phylogeny, and growth of cold-adapted picoprasinophytes in arctic seas. J Phycol 43:78–89
Marie D, Shi XL, Rigaut-Jalabert F, Vaulot D (2010) Use of flow cytometric sorting to better assess the diversity of small photosynthetic eukaryotes in the English Channel. FEMS Microbiol Ecol 72:165–178
Mayers KMJ, Poulton AJ, Daniels CJ, Wells SR and others (2019) Growth and mortality of coccolithophore during spring in a temperate Shelf Sea (Celtic Sea, April 2015). Prog Oceanogr 177:101928
Mayers KMJ, Poulton AJ, Bidle K, Thamatrakoln K and others (2020) The possession of coccoliths fails to deter microzooplankton grazers. Front Mar Sci 7:1–12
Mayers KMJ, Lawrence J, Sandnes Skaar K, Töpper JP and others (2021) Removal of large viruses and their dispersal through fecal pellets of the appendicularian *Oikopleura dioica* during *Emiliania huxleyi* bloom conditions. Limnol Oceanogr 66:3963–3975
Mayers KMJ, Kuhlisch C, Basso JTR, Saltvedt MR, Buchan A, Sandaa RA (2023) Grazing on marine viruses and its biogeochemical implications. MBio 14:e01921-21
Monger BC, Landry MR, Brown SL (1999) Feeding selection of heterotrophic marine nanoflagellates based on the surface hydrophobicity of their picoplankton prey. Limnol Oceanogr 44:1917–1927
Mordecai GJ, Verret F, Highfield A, Schroeder DC (2017) Schrödinger's Cheshire Cat: Are haploid *Emiliania huxleyi* cells resistant to viral infection or not? Viruses 9:51
Morison F, Menden-Deuer S (2015) Early spring phytoplankton dynamics in the subpolar North Atlantic: the influence of protistan herbivory. Limnol Oceanogr 60: 1298–1313
Morison F, Menden-Deuer S (2017) Doing more with less? Balancing sampling resolution and effort in measurements of protistan growth and grazing-rates. Limnol Oceanogr Methods 15:794–809
Nagasaki K, Tomaru Y, Takao Y, Nishida K, Shirai Y, Suzuki H, Nagumo T (2005) Previously unknown virus infects marine diatom. Appl Environ Microbiol 71:3528–3535
Nagata T, Kirchman DL (1992) Release of macromolecular organic complexes by heterotrophic marine flagellates. Mar Ecol Prog Ser 83:233–240
Nejstgaard JC, Frischer ME, Simonelli P, Troedsson C and others (2008) Quantitative PCR to estimate copepod feeding. Mar Biol 153:565–577
Not F, Latasa M, Marie D, Cariou T, Vaulot D, Simon N (2004) A single species, *Micromonas pusilla* (Prasinophyceae), dominates the eukaryotic picoplankton in the Western English Channel. Appl Environ Microbiol 70:4064–4072
Oksanen J, Simpson G, Blanchet F, Kindt R and others (2022) vegan: community Ecology Package, R package version 2.6-4. https://CRAN.R-project.org/package=vegan
Pagarete A, Allen MJ, Wilson WH, Kimmance SA, de Vargas C (2009) Host–virus shift of the sphingolipid pathway along an *Emiliania huxleyi* bloom: survival of the fattest. Environ Microbiol 11:2840–2848
Pasulka AL, Samo TJ, Landry MR (2015) Grazer and viral impacts on microbial growth and mortality in the southern California Current Ecosystem. J Plankton Res 37:320–336
Paulino AI, Egge JK, Larsen A (2008) Effects of increased atmospheric CO_2 on small and intermediate sized osmotrophs during a nutrient induced phytoplankton bloom. Biogeosciences 5:739–748
Poulton AJ, Painter SC, Young JR, Bates NR and others (2013) The 2008 *Emiliania huxleyi* bloom along the Patagonian Shelf: ecology, biogeochemistry, and cellular calcification. Global Biogeochem Cycles 27:1023–1033
Pree B, Kuhlisch C, Pohnert G, Sazhin AF and others (2016) A simple adjustment to test reliability of bacterivory rates derived from the dilution method. Limnol Oceanogr Methods 14:114–123
Schmoker C, Hernandez-Leon S, Calbet A (2013) Microzooplankton grazing in the oceans: impacts, data variability, knowledge gaps and future directions. J Plankton Res 35: 691–706
Staniewski MA, Short SM (2018) Methodological review and meta-analysis of dilution assays for estimates of virus- and grazer-mediated phytoplankton mortality. Limnol Oceanogr Methods 16:649–668
Suttle CA (2005) Viruses in the sea. Nature 437:356–361
Tarran GA, Heywood JL, Zubkov MV (2006) Latitudinal changes in the standing stocks of nano- and picoeukaryotic phytoplankton in the Atlantic Ocean. Deep Res Part II Top Stud Oceanogr 53:1516–1529
Thingstad TF (2000) Elements of a theory for the mechanisms controlling abundance, diversity, and biogeo-

chemical role of lytic bacterial viruses in aquatic systems. Limnol Oceanogr 45:1320–1328

Tyrrell T, Merico A (2004) *Emiliania huxleyi* bloom observations and the conditions that induce them. In: Thierstein HR, Young JR (eds) Coccolithophores: from molecular processes to global impact. Springer, Berlin, p 75–97

Vardi A, Van Mooy BAS, Fredricks HF, Popendorf KJ, Ossolinski JE, Haramaty L, Bidle KD (2009) Viral glycosphingolipids induce lytic infection and cell death in marine phytoplankton. Science 326:861–865

Vardi A, Haramaty L, Van Mooy BAS, Fredricks HF, Kimmance SA, Larsen A, Bidle KD (2012) Host–virus dynamics and subcellular controls of cell fate in a natural coccolithophore population. Proc Natl Acad Sci USA 109: 19327–19332

Vincent F, Gralka M, Schleyer G, Schatz D and others (2023) Viral infection switches the balance between bacterial and eukaryotic recyclers of organic matter during coccolithophore blooms. Nat Commun 14:510

Widdicombe CE, Eloire D, Harbour D, Harris RP, Somerfield PJ (2010) Long-term phytoplankton community dynamics in the Western English Channel. J Plankton Res 32:643–655

Wilhelm SW, Suttle CA (1999) Viruses and nutrient cycles in the sea: viruses play critical roles in the structure and function of aquatic food webs. Bioscience 49:781–788

Wilson WH, Tarran GA, Schroeder D, Cox M, Oke J, Malin G (2002) Isolation of viruses responsible for the demise of an *Emiliania huxleyi* bloom in the English Channel. J Mar Biol Assoc UK 82:369–377

Winter A, Henderiks J, Beaufort L, Rickaby REM, Brown CW (2014) Poleward expansion of the coccolithophore *Emiliania huxleyi*. J Plankton Res 36:316–325

Zhu F, Massana R, Not F, Marie D, Vaulot D (2005) Mapping of picoeucaryotes in marine ecosystems with quantitative PCR of the 18S rRNA gene. FEMS Microbiol Ecol 52: 79–92

Zwirglmaier K, Spence E, Zubkov MV, Scanlan DJ, Mann NH (2009) Differential grazing of two heterotrophic nanoflagellates on marine *Synechococcus* strains. Environ Microbiol 11:1767–1776

Editorial responsibility: Michaela Salcher, České Budějovice, Czech Republic
Reviewed by: 2 anonymous referees

Submitted: September 1, 2023
Accepted: August 26, 2024
Proofs received from author(s): September 30, 2024